

Crystal Structures and Phase Equilibria in the Hafnium-Palladium System

Judith K. Stalick and Richard M. Waterstrat

(Submitted March 17, 2016; in revised form April 26, 2016; published online May 18, 2016)

Portions of the Hf-Pd phase diagram have been reinvestigated in an attempt to resolve contradictions that occur between two previous studies. Techniques employed include Rietveld refinement using x-ray and high-temperature neutron diffraction data to determine crystal structures and phase equilibria. The compound Hf_2Pd_3 was discovered with the Os_2Al_3 structure type, and no evidence was found for a reported “ Hf_3Pd_4 ” phase. More importantly, the compound HfPd_2 was found to be involved in a previously undetected peritectic reaction at 1850 °C. Crystallographic data are given for all compounds encountered, and a significantly revised phase diagram is proposed.

Keywords alloys, binary system, crystal structure, intermetallic compound, phase equilibria, phase transitions

1. Introduction

The Hf-Pd phase diagram which is presented to us today is essentially identical to that proposed by Shurin and Pet'kov in 1972.^[1] In 1994 a thermodynamic study by Selhaoui et al.^[2] contradicted some of the previous results, yet although the phase diagram has been redrawn with minor revisions,^[3–5] it has never been reinvestigated. We summarize the contradictions and results that need further clarification as follows:

- (A) *Composition of the “ Hf_3Pd_4 ” phase.* Reference 1 reports the formation of the compound Hf_3Pd_4 , but suggests parenthetically that its composition may extend to Hf_2Pd_3 . Reference 2 claims that Hf_3Pd_4 exists at 1027 °C and is retained at room temperature. The crystal structure of this phase was unknown. Recently, Hart et al. predicted the existence of a stable Hf_2Pd_3 phase with the Ti_2Pd_3 structure type, based upon computational first principles.^[6]
- (B) *Low temperature stability of HfPd_2 .* Reference 1 claims that a eutectoid reaction occurs at 1370 °C which causes the compound HfPd_2 to decompose at lower temperatures, while Ref 2 states that the enthalpy of formation of HfPd_2 seems exothermic enough to allow this compound to be stable even at

room temperature. They report annealing a sample of HfPd_2 for three days at 1300 K (1027 °C) without decomposition.

- (C) *High temperature stability of HfPd_2 .* Reference 1 indicates that the compound HfPd_2 is stable between 1370 °C and 2075 °C, whereas Ref 2 reports finding 50% HfPd_3 and a small amount of HfPd in their sample of HfPd_2 which they claim are the reaction products of a peritectic reaction presumably occurring somewhere between 1610 °C and 2075 °C.
- (D) *Reaction mechanism of HfPd_2 .* Reference 1 claims that the compound HfPd_2 melts congruently at 2075 °C, while Ref 2 states that the observed reaction products imply that HfPd_2 decomposes peritectically.
- (E) *Reaction mechanism of HfPd_3 .* Reference 1 reports that HfPd_3 melts peritectically at 1965 °C, while Ref 2 suggests that HfPd_3 melts congruently based on the observed reaction products.

The purpose of our present study is to present new measurements which may help to resolve these contradictions, primarily using high-temperature neutron Rietveld refinement and melting point measurements. Our results indicate that a major revision of the Pd-rich portion of the Hf-Pd phase diagram is needed.

2. Experimental Procedures

The procedures used in this study were essentially the same as those described in our previous study of the Hf-Pt system.^[7] Our samples were arc-melted combinations of iodide-process (crystal bar) hafnium and palladium sheets of 1.6 mm thickness and 99.95% purity. All samples with the exception of HfPd were arc-cast into a copper mold to produce rods of 0.635 cm (1/4 in.) diameter and 5 cm to 8 cm in length, then rapidly cooled, to yield samples more suitable for neutron diffraction studies. Weight losses during

Judith K. Stalick, NIST Center for Neutron Research, National Institute of Standards and Technology, Gaithersburg, MD 20899; Richard M. Waterstrat, Materials Science and Engineering Division, National Institute of Standards and Technology, Gaithersburg, MD 20899. Contact e-mail: judith.stalick@nist.gov.

melting did not exceed 1% but significant losses of Pd could occur by vaporization if the samples were heated in a vacuum above 1000 °C. In order to reduce these losses we therefore eliminated our customary prior homogenization annealing, and followed the homogenization directly as it unfolded during collection of powder neutron diffraction data using a high-vacuum furnace. All neutron diffraction patterns were obtained using the Cu(311) monochromator ($\lambda = 1.5401(2)$ Å) of the BT-1 32-detector high-resolution powder diffractometer at the NIST Center for Neutron Research; the data were corrected for absorption, and structural Rietveld refinements were carried out using the GSAS suite of programs^[8] with EXPGUI interface.^[9] The HfPd sample was contained in a vanadium sample holder (which does not significantly add to the diffracted intensities); the sample was rotated during data collection at room temperature in order to minimize the effects of the irregular sample geometry.

3. Results and Discussion

We describe here the behavior on heating of samples of the nominal compositions Hf₅₀Pd₅₀ (HfPd), Hf₄₃Pd₅₇ (“Hf₃Pd₄”), Hf₄₀Pd₆₀ (Hf₂Pd₃), and Hf₃₃Pd₆₇ (HfPd₂). The crystallographic results presented in the following sections are summarized in Table 1, along with data on other known Hf-Pd compounds.^[10-13]

3.1 HfPd

Declairieux et al.^[11] reported that HfPd is isostructural with NiTi (B19'-type) at compositions up to Hf₄₈Pd₅₂, and undergoes a martensitic transformation at around 773 K (500 °C). The reported lattice parameters ($a = 3.3$ Å, $b = 4.38$ Å, $c = 5.4$ Å, $\beta = 107.2^\circ$), when transformed to a standard crystallographic setting using the matrix $[-1 \ 0 \ 0/0 \ -1 \ 0/1 \ 0 \ 1]$, are $a = 3.3$ Å, $b = 4.38$ Å, $c = 5.38$ Å, $\beta = 107.5^\circ$ and correspond well with those found in this study (Table 1); detailed refinement results are presented in Table 2. Upon heating above 600 °C, we observed a transition to a CsCl (B2) structure type, with $a = 3.3279(5)$ Å at

700 °C. Data collected on cooling substantiate the hysteresis reported in Ref 11; the mass fraction of B2 phase was 100% at 600 °C, 75% at 560 °C, and 50% at 540 °C. Refinement results using data collected at 700 °C are given in Table 3.

Xing et al.^[14] and Hart et al.^[6] predict that HfPd should have a B33-type (CrB-type) structure at room temperature based upon first principles calculations. In fact, the B19'-type structure determined here represents only a very slight monoclinic distortion from the orthorhombic B33 structure type. Using our neutron diffraction data, the HfPd structure can be refined as orthorhombic B33-type, space group *Cmcm* (63), resulting in lattice parameters $a = 3.2886(6)$ Å, $b = 10.209(1)$ Å, $c = 4.3660(7)$ Å, and yielding essentially the same coordination polyhedra as does the monoclinic structural model. However, the Rietveld agreement factors for the orthorhombic model ($\chi^2 = 2.0$ and $R_{wp} = 0.065$) are significantly higher than those for the monoclinic model ($\chi^2 = 1.3$ and $R_{wp} = 0.051$), indicating that the monoclinic model is to be preferred. In either model of the HfPd structure, the Hf atom is 15-coordinate (8 Hf-Hf distances of 3.29 to 3.66 Å, and 7 Hf-Pd distances of 2.75-2.88 Å) and the Pd atom is 9-coordinate (2 Pd-Pd distances of 2.82 Å and 7 Pd-Hf distances of 2.75-2.88 Å). The prototype structure of NiTi has a much greater monoclinic distortion, which results in 14-coordinate Ti atoms and 12-coordinate Ni atoms.^[15]

In our previous study of the structure and phase transformations in ZrPd,^[16] monoclinic symmetry for the compound ZrPd was indicated based on electron diffraction data, but the distortion was too small to refine using our neutron powder diffraction data. In light of the similarities between Hf and Zr compounds, it seems probable that ZrPd also possesses the NiTi structure type at room temperature. The reported orthorhombic lattice parameters ($a = 3.3305$ Å, $b = 10.304$ Å, $c = 4.3745$ Å) can be transformed to the monoclinic setting using the matrix $[-1 \ 0 \ 0/0 \ 0 \ 1/2 \ 1/2 \ 0]$ to give $a = 3.3305$ Å, $b = 4.3745$ Å, $c = 5.4144$ Å, $\beta = 107.91^\circ$ for ZrPd.

3.2 Hf₂Pd₃ and “Hf₃Pd₄”

Our original goal was to prepare a sample of the compound Hf₃Pd₄ and determine its crystal structure. At

Table 1 Crystallographic data for Hf-Pd compounds

Compound	Space group	Structure type	a , Å	b , Å	c , Å	β , °	Z	T , °C	References
Hf ₂ Pd	<i>I4/mmm</i> (139)	Zr ₂ Cu(*)	3.251(1)	...	11.061(2)	...	2	22	12
HfPd	<i>P2₁/m</i> (11)	NiTi, B19'	3.2895(4)	4.3666(6)	5.3509(7)	107.38(1)	2	22	This work
...	3.30	4.38	5.38	107.5	11(**)
HfPd (ht)	<i>Pm$\bar{3}m$</i> (221)	CsCl, B2	3.3279(5)	1	700	This work
Hf ₂ Pd ₃	<i>I4/mmm</i> (139)	Os ₂ Al ₃	3.4142(4)	...	14.765(2)	...	2	22	This work
HfPd ₂	<i>I4/mmm</i> (139)	MoSi ₂	3.3965(4)	...	8.6570(8)	...	2	22	This work
...	3.399	...	8.658	10
HfPd ₃	<i>P6₃/mmc</i> (194)	Ni ₃ Ti	5.595	...	9.192	...	4

Standard uncertainties are given in parentheses, and include uncertainty in the neutron wavelength. (*) Reported as MoSi₂ type in Ref. 12 (**) After transformation to standard crystallographic setting

Table 2 Results of room-temperature Rietveld refinement for HfPd

Atom	Site	<i>x</i>	<i>y</i>	<i>z</i>	<i>U</i> _{iso} , Å ³
Pd	2e	0.0831(10)	0.25	0.6745(3)	0.0157(4)
Hf	2e	0.3613(8)	0.25	0.2128(3)	0.0125(4)

$\chi^2 = 1.3$, $R_{wp} = 0.051$. $P2_1/m$, $Z = 2$, $a = 3.2895(5)$ Å, $b = 4.3666(6)$ Å, $c = 5.3509(7)$ Å, $\beta = 107.38(1)^\circ$. Interatomic distances (Å): Pd atom [CN = 9]: Pd-Pd 2.819(2)×2; Pd-Hf 2.749(2), 2.792(2)×2, 2.795(2)×2, 2.870(3), 2.880(3). Hf atom [CN = 15]: Hf-Hf 3.2895(5)×2, 3.468(3)×2, 3.517(3)×2, 3.656(2)×2; Hf-Pd 2.749(2), 2.792(2)×2, 2.795(2)×2, 2.870(3), 2.880(3). Standard uncertainties are given in parentheses, and include uncertainty in the neutron wavelength

Table 3 Results of Rietveld refinement for HfPd (ht) at 700 °C

Atom	Site	<i>x</i>	<i>y</i>	<i>z</i>	<i>U</i> _{iso} , Å ³
Hf	1a	0.0	0.0	0.0	0.0280(5)
Pd	1b	0.5	0.5	0.5	0.0508(9)

Atoms	Distance, Å
Hf-Hf	3.3279(5) × 6
Hf-Pd	2.8820(4) × 8

$\chi^2 = 1.0$, $R_{wp} = 0.081$. $Pm\bar{3}m$, $Z = 1$, $a = 3.3279(5)$ Å. Standard uncertainties are given in parentheses, and include uncertainty in the neutron wavelength

that time, there was little doubt of its existence. The isoelectronic counterparts Zr_3Pd_4 , Zr_3Pt_4 , and Hf_3Pt_4 had been discovered recently and had been identified as possessing a Pu_3Pd_4 -type structure at or slightly above room temperature.^[7,17,18] Furthermore, the existence of Hf_3Pd_4 at 1027 °C had been confirmed and it was reported that it could be retained at room temperature.^[2] Our first sample, therefore, had the composition Hf_3Pd_4 and was homogenized for several hours under vacuum at 1400 °C. Neutron diffraction data were subsequently collected while heating the sample slowly up to 1100 °C under high vacuum; at this point the sample was found to consist of two phases: Hf_2Pd_3 , isostructural with Ti_2Cu_3 (Os_2Al_3 -type), and a B2-type structure with $a = 3.332(1)$ Å which was assumed to be the high-temperature form of HfPd. The mass fraction of the B2 phase increased from 40% at 1100 °C to 52% at 1200 °C and 67% at 1300 °C; the total elapsed time for data collection at these three temperatures was ≈14 h. When the temperature was raised to 1400 °C, the sample melted completely even though it had previously been homogenized at this temperature. This led us to the realization that our sample was losing Pd by vaporization; examination of the vacuum apparatus after cooling showed that a metallic substance had been plated on the inside of the vacuum tubing. The existing phase diagram^[1] indicates that Hf-Pd alloys containing less than an atomic fraction of 50% Pd will melt at ≈1415 °C and alloys containing less than ≈33% Pd will melt eutectically at ≈1325 °C.

Our experiment had clearly shown us that HfPd and Hf_2Pd_3 are the equilibrating phases at temperatures between 1000 and 1300 °C and that no Hf_3Pd_4 was forming in this region. It now seemed necessary to prepare a new sample containing an atomic fraction of 60% Pd (Hf_2Pd_3) and take

measures to reduce the losses of Pd by vaporization. We did this by eliminating our customary high-temperature homogenization treatment and beginning collection of neutron diffraction data using a sample in the “as cast” condition, enabling the observation of the state of homogenization and adjusting temperatures accordingly. By using these modified procedures we were able to produce a sample of Hf_2Pd_3 in an essentially phase-pure condition.

Analysis of initial neutron powder data at room temperature on the sample of composition Hf_2Pd_3 showed mostly the Os_2Al_3 -type phase, with preferred orientation effects on the intensities, along with some poorly-crystalline additional phases. The sample was heated rapidly to 1100 °C in the high-vacuum furnace; after 1 h at 1100 °C most impurity peaks were gone, and the sample remained essentially phase-pure on gradual cooling as monitored by the neutron diffraction intensities. Data were then collected at room temperature for Rietveld refinement.

The Os_2Al_3 structure type was confirmed, and the final structural parameters are given in Table 4. The agreement between calculated and observed intensities is presented in Fig. 1. Two other structural models were also considered: the Ti_2Pd_3 structure type predicted by Hart et al.,^[6] space group $Cmcm$ (no. 63), as was found for Hf_2Pt_3 ^[19] and the Ti_2Cu_3 -type structure (space group $P4/nmm$, no. 129) as reported by Schubert et al.^[20] and listed as a type structure in Pearson.^[15] The Ti_2Pd_3 structure type, which was also reported for the low-temperature form of Ti_2Ni_3 ,^[21] results from a small distortion of the tetragonal Os_2Al_3 lattice. This model did not improve the fit of the calculated and observed intensities, and the refined structural parameters were identical to those reported here within their standard uncertainties. The Ti_2Cu_3 -type model behaved similarly,

except that the refinement was very unstable owing to extreme correlations among the refined parameters. It is worth noting that Ti_2Cu_3 has also been reported as belonging to the Os_2Al_3 structure type^[22]; it is possible that Ti_2Cu_3 is not a valid structure type.

3.3 HfPd₂

The phase diagram reported by Shurin and Pet'kov^[1] indicates that the compound HfPd₂ is stable only above 1370 °C and that it will decompose eutectoidally below that temperature. Phase diagram computations performed by Selhaoui et al.,^[2] based on their own measurements have, however, led them to conclude that its enthalpy of formation seemed exothermic enough for HfPd₂ to be stable at room temperature. Accordingly, they annealed a sample of HfPd₂ for 3 days at 1027 °C and observed no decomposition.

We prepared an arc-cast sample of HfPd₂ whose structure was consistent with the MoSi₂ structure type but contained a small percentage of impurities at room temperature. Rietveld refinement of the structure indicated significant preferred orientation of the crystallites. The sample was heated to 1100 °C at the rate of 600 °C/h under high vacuum, and held for slightly more than 2 h while collecting neutron diffraction data; subsequent data sets were collected

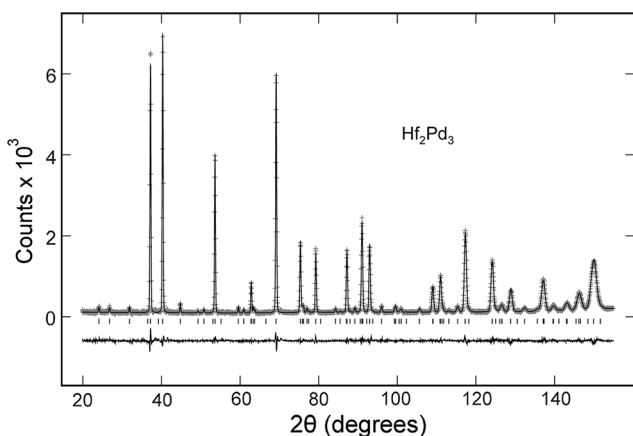


Fig. 1 Observed (+), calculated (solid line) and difference patterns for the neutron Rietveld refinement of Hf₂Pd₃ at room temperature ($\lambda = 1.5401 \text{ \AA}$). Hash marks indicate calculated positions for the reflections

at 900, 700, 500 and 300 °C followed by slow cooling to room temperature. Most impurity peaks disappeared on heating to 1100 °C and no significant changes were observed that suggested decomposition at any of these temperatures. A final data set was later obtained at room temperature.

Neutron Rietveld refinement of the structure at room temperature confirmed the MoSi₂ structure type, along with a mass fraction of $\approx 2\%$ HfPd₃. The diffraction pattern still showed the effects of preferred orientation of the crystallites, which was modelled using a spherical harmonics function. Final refinement results are given in Table 5.

3.4 HfPd₃

Although no samples of composition HfPd₃ were prepared for this study, the detection and successful inclusion of this impurity phase in the Rietveld refinement of the HfPd₂ sample (section 3.3) confirms the hexagonal TiNi₃-type structure reported by Dwight and Beck.^[13] The refined lattice parameters $a = 5.598(2) \text{ \AA}$ and $c = 9.183(6) \text{ \AA}$ are in good agreement with those given in Table 1.

3.5 Solidus Temperatures for HfPd₂ and HfPd₃

The report by Shurin and Pet'kov^[1] that the compound HfPd₂ melts congruently at 2075 °C and that HfPd₃ melts peritectically at 1965 °C was based on DTA measurements. Selhaoui et al.^[2] have analyzed the reaction products that they observed in their samples of HfPd₂ and HfPd₃ and have stated that their observations are probably in contradiction with those of Shurin and Pet'kov. They propose that their observation of HfPd₃ and HfPd in the transformation products of their sample of HfPd₂ suggests that HfPd₂ melts peritectically while HfPd₃ melts congruently. If this is correct, then it should be the compound HfPd₃, not HfPd₂, that melts at 2075 °C. In order to resolve these discrepancies, we have therefore undertaken to measure, by direct observation, the temperature at which liquid appears in HfPd₂ on heating.

Our sample was part of the 0.635 cm (1/4 in.) diameter arc-cast rod that was intended for the neutron diffraction study. A small (2 cm long) piece had broken off the end of the rod as it was cooled. Its fracture surface was seen to be composed of columnar crystals arranged in a concentric pattern with a high degree of preferred orientation. As

Table 4 Results of room-temperature Rietveld refinement for Hf₂Pd₃

Atom	Site	x	y	z	$U_{\text{iso}}, \text{ \AA}^3$
Pd(1)	2a	0.0	0.0	0.0	0.0178(7)
Pd(2)	4e	0.0	0.0	0.1967(1)	0.0121(4)
Hf	4c	0.0	0.0	0.3899(1)	0.0096(3)

Standard uncertainties are given in parentheses, and include uncertainty in the neutron wavelength. $\chi^2 = 1.7$, $R_{\text{wp}} = 0.077$. $I4/mmm$, $Z = 2$, $a = 3.4142(4) \text{ \AA}$, $c = 14.765(2) \text{ \AA}$. Interatomic distances (\AA): Pd(1) [CN = 10]: Pd(1)-Pd(2) 2.904(2) \times 2; Pd(1)-Hf 2.911(1) \times 8. Pd(2) [CN = 10]: Pd(2)-Pd(1) 2.904(2); Pd(2)-Pd(2) 2.883(2) \times 4; Pd(2)-Hf 2.853(2), 2.731(1) \times 4. Hf [CN = 14]: Hf-Hf 3.4142(4) \times 4, 3.253(2); Hf-Pd(1) 2.911(1) \times 4; Hf-Pd(2) 2.853(2), 2.731(1) \times 4

Table 5 Results of room-temperature Rietveld refinement for HfPd₂

Atom	Site	x	y	z	$U_{\text{iso}}, \text{\AA}^3$
Hf	2a	0.0	0.0	0.0	0.0078(3)
Pd	4e	0.0	0.0	0.3368(2)	0.0120(3)

Standard uncertainties are given in parentheses, and include uncertainty in the neutron wavelength. $\chi^2 = 2.3$, $R_{\text{wp}} = 0.088$. $I4/mmm$, $Z = 2$, $a = 3.3965(4) \text{\AA}$, $c = 8.6570(8) \text{\AA}$. Interatomic distances (\AA): Pd atom [CN = 10]: Pd-Pd 2.825(4), 2.833(2) $\times 4$; Pd-Hf 2.916(2), 2.786(1) $\times 4$. Hf atom [CN = 14]: Hf-Hf 3.3965(4) $\times 4$; Hf-Pd 2.916(2) $\times 2$, 2.786(1) $\times 8$

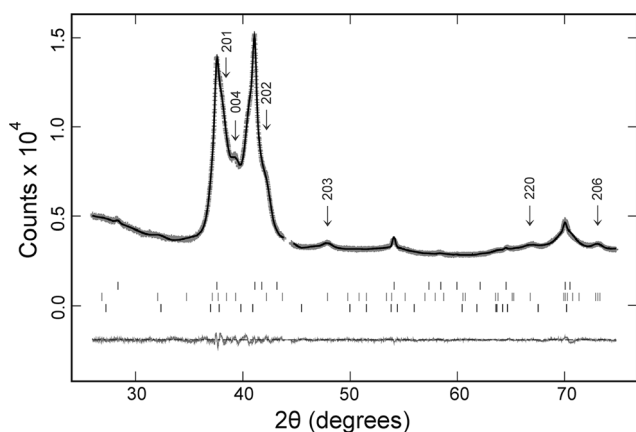


Fig. 2 Rietveld fit of x-ray pattern of HfPd₂ after partial melting at 1850 °C followed by rapid cooling (Cu K α , $\lambda = 1.5406 \text{\AA}$). The lower hash marks indicate calculated positions for Hf₂Pd₃ reflections, the middle hash marks indicate those for HfPd₃, and the upper hash marks indicate calculated positions for the original un-melted HfPd₂ phase. Arrows indicate indexing of the strongest reflections for the HfPd₃ phase

indicated in section 3.3, this sample became nearly phase pure HfPd₂ (MoSi₂ type) upon heating to 1100 °C.

The small as-cast sample was placed on a flat, polished disc of hot-pressed HfO₂ located on top of a Ta holder so that the HfPd₂ sample did not come into contact with the Ta holder. The entire assembly was placed in a high-vacuum furnace and heated quickly to 1600 °C, then held for about 1 min to insure temperature homogeneity. It was then heated slowly until the sample collapsed abruptly at 1850 °C when partial melting had occurred. Subsequent examination of the partially melted sample showed that it had wet the HfO₂ substrate and had adhered to it. However, it separated cleanly from the substrate and did not appear to have chemically reacted with it, nor had the sample contacted the Ta holder.

X-ray diffraction indicated that the sample had been in the process of transforming peritectically according to the reaction HfPd₂ \rightarrow Liquid + HfPd₃. Powder x-ray diffraction data were obtained, using Cu K α radiation, on a ground portion of the partially melted and rapidly cooled sample. Rietveld refinement indicated that the sample now consisted of approximate mass fractions of 65% Hf₂Pd₃, 30% HfPd₃, and 5% HfPd₂ (presumably from an original un-melted portion of the sample). The formerly single phase HfPd₂ sample now showed clear evidence for the presence of

HfPd₃ (see Fig. 2) and thus for the existence of a peritectic reaction at 1850 °C above which HfPd₂ becomes unstable. Therefore, HfPd₂ cannot be involved in a congruent reaction at 2075 °C as indicated in Ref 1 because it does not exist at that temperature.

When Shurin and Pet'kov^[1] reported that the compound HfPd₂ melts congruently at 2075 °C, they were apparently unaware that HfPd₂ does not exist above 1850 °C. The question then arises as to what they were actually detecting when they received a DTA signal at this temperature. It appears (see Fig. 3) that their sample probably consisted of two phases: a liquid Hf-Pd solution and the solid compound HfPd₃. The source of their signal must therefore be the HfPd₃ phase. However, the lower temperature (1965 °C) which they reported for their HfPd₃ sample implies that the congruent maximum does not occur at the stoichiometric composition assuming, of course, that the sample composition is not changing significantly during the measurement. We have found that losses of Pd by vaporization can be kept within acceptable limits in our high-vacuum furnace if our measurements are completed within a time frame of several minutes at temperatures as high as 1800 °C. We expect that Shurin and Pet'kov could have made accurate measurements as high as 2100 °C because their experiments were done in an inert atmosphere rather than in a high vacuum.

Liquidus and solidus boundaries merge tangentially as they pass through a congruent maximum, however, and their trajectories are quite flat in this region. Therefore, we are safe in assuming that the temperature of the congruent maximum in HfPd₃ is close to that of the liquidus temperature in HfPd₂ and perhaps occurs at a slightly higher temperature. A comparison of the solidus temperatures of the isoelectronic systems Zr-Pd^[23] and Hf-Pd is given in Table 6, and suggests that this is a reasonable assumption. We thus conclude that the highest-melting compound in the Hf-Pd system is most likely HfPd₃ rather than HfPd₂.

3.6 Proposed Modifications to the Hf-Pd Phase Diagram

We are proposing the following modifications to the Hf-Pd phase diagram, in an attempt to resolve the contradictions between references^[1,2] as presented in the Introduction:

- (A) *Composition of the "Hf₃Pd₄" phase.* Our study suggests that this phase has the composition Hf₂Pd₃ as predicted from first principles calculations,^[6] in agreement with the alternative stoichiometry suggested by Ref 1; this compound was found to have the Os₂Al₃

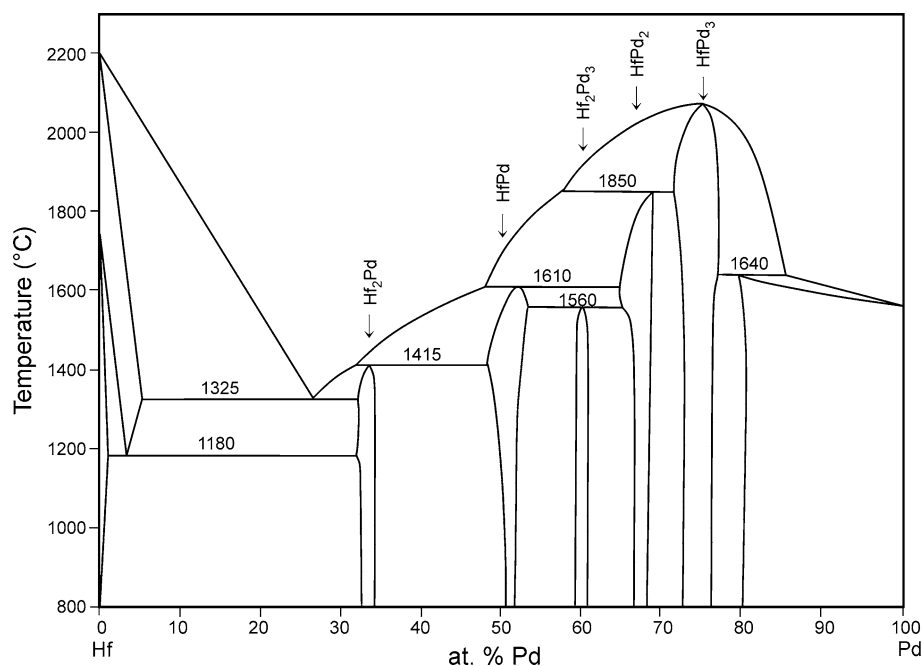


Fig. 3 Hf-Pd phase diagram modified according to our newly acquired data. Phase boundaries have not been experimentally determined

Table 6 Solidus temperatures of isomorphous AB_2 and AB_3 compounds in the Zr-Pd and Hf-Pd systems

	Reference 23		This study	Reference 1
ZrPd ₂	1610 °C [P]	HfPd ₂	1850 °C [P]	2075 °C [C] [†]
ZrPd ₃	1890 °C [C]	HfPd ₃	2075 °C [C] ^(*)	1965 °C [P] [†]

[P]: peritectic transformation; [C]: congruent transformation. (*) Assumed value. Authors (Ref 1) report this value for the compound HfPd₂ (see text). [†]We have shown that these values are incorrect, presumably due to misinterpretation of DTA measurements in Ref 1

structure type. We found no evidence for the existence of a compound with stoichiometry Hf₃Pd₄.¹

- (B) *Low temperature stability of HfPd₂*. Our measurements support Ref. 2 We have found no evidence that HfPd₂ decomposes eutectoidally below 1370 °C. We propose extending the range of stability of HfPd₂ to 800 °C, and possibly to room temperature. The absence of any evidence for a eutectoidal decomposition in this study and in an HfPd₂ sample annealed at 1027 °C for 3 days^[2] may conceivably result from sluggish kinetics. If so, then it would be necessary to anneal these samples for long periods of time in order to provide a definitive answer to this question.
- (C) *High temperature stability of HfPd₂*. Our study supports the results of Ref. 2 The stability of the compound HfPd₂ extends no higher than 1850 °C, where it terminates in a peritectic reaction. The stability of

the compound HfPd₃ extends above 1850 °C.

- (D) *Reaction mechanism of HfPd₂*. We again support the results of Ref. 2 Above 1850 °C the compound HfPd₂ is replaced by a two-phase equilibrium mixture of a liquid solution and the solid compound HfPd₃. The DTA signal reported as a congruent melting of HfPd₂ in Ref 1 has apparently been misinterpreted and is actually the liquidus boundary at this composition.
- (E) *Reaction mechanism of HfPd₃*. We support the conclusion of Ref 2 that HfPd₃ melts congruently. However, the maximum melting temperature may not correspond to the stoichiometric composition. The highest temperature measured in the Hf-Pd system by Ref 1 is 2075 °C and seems likely to be close to the maximum. We did not attempt to measure the melting point of this compound, however, because our equipment operates only under vacuum where we believe that losses of Pd by vaporization would become excessive over 2000 °C.

¹Our data do not preclude the existence of a metastable phase near the composition Hf₃Pd₄. Some small impurity peaks in the sample of composition Hf₂Pd₃ were found, representing a mass fraction of ≈ 2% or less; larger amounts of the same impurity peaks existed initially in the sample of nominal composition Hf₃Pd₄.

In addition to the resolution of conflicting reports from the literature, we find it unrealistic to portray all compounds

as line compounds with fixed compositions. We prefer instead to portray them with ranges of composition similar (but not identical) to those observed in the Zr-Pd system.^[23]

A suggested Hf-Pd phase diagram is presented in Fig. 3.

4. Conclusion

We have shown that several portions of the currently accepted Hf-Pd phase diagram are seriously in error. Although we did not include the entire composition range of the Hf-Pd phase diagram in this study, we feel that the proposed modifications outlined herein should be enough information to warrant a major revision of the Pd-rich portion.

Acknowledgments

We were fortunate in having the very capable assistance of Anthony Giuseppetti in arc-casting our samples and in measuring our high-temperature melting points. We also thank Sandy Claggett for preparing our metallographic samples, Maureen Williams for x-ray diffraction measurements, and Juscelino Leão for his assistance with the high-temperature furnace for the collection of neutron data.

References

1. A.K. Shurin and V.V. Pet'kov, The Hf-Pd Equilibrium Diagram, *Russ. Metall. (Engl. Transl.)*, 1972, **2**, p 122-124
2. N. Selhaoui, J.C. Gachon, and J. Hertz, Thermodynamic Study of the Pd-Hf System by High-Temperature Calorimetry, *J. Alloys Compd.*, 1994, **204**, p 157-164
3. S.N. Tripathi and S.R. Bharadwaj, The Hf-Pd (Hafnium-Palladium) System, *J. Phase Equilib.*, 1995, **16**, p 527-531
4. H. Okamoto, *Binary Alloy Phase Diagrams*, 2nd ed., Vol 2, T.B. Massalski, H. Okamoto, P.N. Subramanian, and I. Kacprzak, Eds., ASM International, Materials Park, 1990, p 2099-2100
5. H. Okamoto, Hf-Pd (Hafnium-Palladium), *J. Phase Equilib.*, 1997, **18**, p 223
6. G.L.W. Hart, S. Curtarolo, T.B. Massalski, and O. Levy, Comprehensive Search for New Phases and Compounds in Binary Alloy Systems Based on Platinum-Group Metals, Using a Computational First Principles Approach, *Phys. Rev. X*, 2013, **3**, p 041035
7. J.K. Stalick and R.M. Waterstrat, The Hafnium-Platinum Phase Diagram, *J. Phase Equilib. Diffus.*, 2014, **35**, p 15-23
8. A.C. Larson and R.B. VonDreele, *General Structure Analysis System (GSAS)*, Los Alamos National Laboratory Report No. LAUR 86-748, 2005
9. B.H. Toby, EXPGUI, a Graphical User Interface for GSAS, *J. Appl. Crystallogr.*, 2001, **34**, p 210-213
10. M.V. Nevitt, Alloy Chemistry, *Electronic Structure and Alloy Chemistry of the Transition Elements*, P.A. Beck, Ed., Interscience, New York, 1962
11. C. Declairieux, P. Vermaut, R. Portier, P. Ochin, V. Kolomytsev, A. Pasko, and G. Monastyrsky, Study of the Martensitic Transformation in the Hafnium-Palladium System, *ESOMAT 2009—8th European Symposium on Martensitic Transformations*, P. Sittner, V. Paidar, L. Heller, and H. Seiner, Eds., Sept. 7-11, 2009 (Prague), 2009, p 04005
12. M.V. Nevitt and J.W. Downey, A Family of Intermediate Phases Having the Si₂Mo-Type Structure, *Trans. Metall. Soc. AIME*, 1962, **224**, p 195-196
13. A.E. Dwight and P.A. Beck, Close-Packed Ordered Structures in Binary AB₃ Alloys of Transition Elements, *Trans. Metall. Soc. AIME*, 1959, **215**, p 976-979
14. W. Xing, X.-Q. Chen, D. Li, Y. Li, C.L. Fu, S.V. Meschel, and X. Ding, First-Principles Studies of Structural Stabilities and Enthalpies of Formation of Refractory Intermetallics: TM and TM₃ (T = Ti, Zr, Hf; M = Ru, Rh, Pd, Os, Ir, Pt), *Intermetallics*, 2012, **28**, p 16-24
15. W.B. Pearson, *The Crystal Chemistry and Physics of Metals and Alloys*, Wiley-Interscience, New York, 1972
16. L.A. Bendersky, J.K. Stalick, R. Portier, and R.M. Waterstrat, Crystallographic Structures and Phase Transformations in ZrPd, *J. Alloys Compd.*, 1996, **236**, p 19-25
17. L.A. Bendersky, J.K. Stalick, and R.M. Waterstrat, Crystal Structure of the Zr₃Pd₄ Phase, *J. Alloys Compd.*, 1993, **201**, p 121-126
18. J.K. Stalick and R.M. Waterstrat, The Zirconium-Platinum Phase Diagram, *J. Alloys Compd.*, 2007, **430**, p 123-131
19. J.K. Stalick, K. Wang, and R.M. Waterstrat, The Crystal Structure and Phase Transition of Hf₂Pt₃, *J. Phase Equilib. Diffus.*, 2013, **34**, p 385-389
20. K. Schubert, H.G. Meissner, and W. Rossteutscher, Eine Strukturdaten metallischer Phasen, *Naturwissenschaften*, 1964, **51**, p 507
21. T. Hara, T. Ohba, K. Otsuka, and M. Nishida, Phase Transformation and Crystal Structures of Ti₂Ni₃ Precipitates in Ti-Ni Alloys, *Mater. Trans.*, 1997, **38**, p 277-284
22. V.N. Eremenko, Y.I. Buyanov, and N.M. Panchenko, Polythermal and Isothermal Sections of the System Titanium-Copper-Silver. Part II, *Sov. Powder Metall. Met. Ceram.*, 1970, **9**, p 410-414
23. R.M. Waterstrat, A. Shapiro, and A. Jeremie, The Palladium-Zirconium Phase Diagram, *J. Alloys Compd.*, 1999, **290**, p 63-70